

A Novel Integration of Hodrick-Prescott Filter and Harmonic Analysis with Machine Learning Methods to Enhance Time Series Prediction Accuracy of Daily and Monthly Wind Speeds


Chigbogu Godwin Ozoegwu (✉ chigbogu.ozoegwu@unn.edu.ng)
University of Nigeria <https://orcid.org/0000-0002-2048-5354>

Research Article

Keywords: wind speed time series, machine learning, Hodrick-Prescott filter, harmonic analysis, artificial neural networks, support vector machines

Posted Date: September 30th, 2021

DOI: <https://doi.org/10.21203/rs.3.rs-794022/v1>

License:  This work is licensed under a Creative Commons Attribution 4.0 International License. [Read Full License](#)

Abstract

In this work, a new hybrid algorithm for modelling time series of daily and monthly wind speed is proposed. The method utilizes Hodrick-Prescott Filter (HPF) to decompose raw wind speed data into trend and cyclic components, and harmonic analysis (HA) is thereafter used to decompose the cyclic component into the periodic and stochastic sub-components. Machine learning (ML) methods are then used to model the time series of both the trend and stochastic components. The predicted wind speeds are finally summed from the individual predictions of the ML methods and harmonic analyses. To highlight the considerably higher predictive accuracy that results from the introduced data pre-treatments with HPF and HA, the proposed hybrid algorithm is compared against the traditional ML methods that are not subjected to the pre-treatments. The proposed hybrid algorithms are highly accurate relative to the traditional ML methods reflecting much higher coefficients of determination and correlation coefficients, and much lower error indices. Artificial neural networks (ANNs), linear regression with interactions (LRI), support vector machine (SVM), rational quadratic Gaussian process regression (RQGPR), fine regression trees (FRTs) and boosted ensembles of trees (BETs) are used as the illustrative machine learning methods. To guarantee both versatility and robustness, the methods are tested on example data drawn from both temperate and tropical conditions.

1. Introduction

Wind energy derives from the kinetic energy of atmospheric air molecules. The heating effects of solar energy absorbed by the earth's surface and atmosphere create atmospheric thermal differential that drives wind. Energy is tapped from wind when the moving air exerts an impulsive torque on a rotor via the rotor blade. In modern times rotors bear an electric generators while in the historic times rotors bore grain grinders, powered a water pumps, etc [1]. Though wind energy exploitation dates back five thousand years, majority of the technological advancement was witnessed in the last thirty years [2] due to growing issues of energy security and environmental protection. The concerns about energy security and environmental protection stimulated research interest in wind energy which has succeeded in shrinking the limitations on wind speed forecasting, wind turbine technology, wind energy policy, etc [3]. Wind energy systems perform best when located in prominent or unobstructed areas like hill-tops and offshore as long as they do not compromise tourism value [4]. According to Keivanpour et al [5], who summarized the results of recent works focusing on potential offshore wind energy around the world, offshore holds stronger and larger wind energy resources than land. Wind energy is increasingly becoming an important renewable resource for power generation globally, and its use is increasing annually [6]. The cost of wind energy has continued to fall as the technology, manufacture, location and maintenance of wind turbine become more standardized and efficient. As a result, the global wind power capacity grew from 74GW to 487GW from 2006 to 2016 while the annual rate of global wind power addition grew from 15% in 2005 and peaked at 64% in 2015 [7]. There are, therefore, prospects of surmounting all the challenges against achieving the global wind power target of 1000 GW by 2030 [2].

Since terrestrial solar energy is intermittent, the arising wind speed is also intermittent thus difficult to model and predict making the decision about optimal wind turbine location a difficult task. The problem of intermittency limits the deployment of wind energy systems in large-scale electricity utilities thus the need for reliable modelling of wind speed. Therefore, research effort has been devoted to improving the accuracy of wind speed prediction. The several ways to predict wind speed include (1) using geographic location and seasonality parameters as predictors, see Fadare [8] who used latitude, longitude and month number as the predictors of wind speed, (2) using meteorological parameters as predictors, see [9, 10] in which air temperature, relative humidity and vapor pressure were used to predict monthly mean daily wind speed, and (3) using historical wind speed data as the predictors, see [11]. Multiple linear regression methods [12, 13], stochastic regression methods [11] and artificial intelligence methods [10] have been used to

correlate these classes of predictors with wind speed. The following review is tailored within the scope of this work by focusing on the application of artificial intelligence in time series modelling and forecasting of wind speed.

Neural networks based on adaptive linear element, back propagation, and radial basis function were found to be comparatively effective in 1-h-ahead wind speed forecasting [14]. Liu et al [11] found that Wavelet Packet-ANN performed best amongst the three hybrid models compared for prediction of half-hourly wind speed. Two methods hybridized from five-three-Hanning weighted average smoothing, ensemble empirical mode decomposition, and nonlinear autoregressive neural networks were shown in [15] to predict ten-minute wind speed data better than the traditional methods like ARIMA and persistent methods. Ensemble empirical mode decomposition was used to preprocess wind speed data for a component-by-component adaptive prediction using wavelet neural networks in [16]. A secondary decomposition algorithm, which combined wavelet packet decomposition and the fast ensemble empirical mode decomposition, was used to improve the capacity for multi-step wind speed prediction of Elman neural networks [17]. The four decomposition algorithms; wavelet decomposition, wavelet packet decomposition, empirical mode decomposition and fast ensemble empirical mode decomposition, were jointly used to improve the accuracy of extreme learning machines in multi-step wind speed forecasting [18]. Fast ensemble empirical mode decomposition was used for data preprocessing in a method that trained regularized extreme learning machine by backtracking search algorithm for forecasting of wind speed in short-term horizons [19]. A combination of non-positive constraint theory, neural networks, nonlinear and linear statistical models and enhanced with a modified cuckoo search algorithm is proposed and found in [20] to be more effective for forecasting wind speed than the hybrid nonlinear or linear single models. A hybrid of support vector regression, stacked de-noising auto-encoder and unscented Kalman filter, which embodied novel filtering approach that combines statistical and numerical weather prediction models, was proposed and validated in [21] to accurately predict wind speed on short- and long-term horizons. In [22], variational mode decomposition was used to decompose wind speed time series into different intrinsic mode functions to reduce non-stationary behaviour. Then, ANN was used to build sub-models from which predicted wind speeds were integrated. The method was seen to perform better than ANNs based on wavelet decomposition, and empirical mode decomposition used earlier in [23, 24]. In a similar study [25], a combination of the complementary ensemble empirical mode decomposition with adaptive noise and the variational mode decomposition was used to decompose original wind speed series into intrinsic mode functions of different frequencies, and an improved AdaBoost.RT algorithm coupled with extreme learning machine was used to forecast the decomposed modes. Another study based on complementary ensemble empirical mode decomposition with adaptive noise improved the accuracy of short-term wind speed forecasting by using ARIMA in selecting the best input variables and implementing an error correction [26]. In [27], complete ensemble empirical mode decomposition was used to reinforce wavelet packet decomposition of wind speed time series before the application of different ANNs for modelling of the components from which the forecasted wind speeds were integrated. Wind speed decomposition with complete ensemble empirical mode decomposition was reinforced with the empirical wavelet transform before the application of ANN that is improved by flower-pollination algorithm for wind speed forecasting [28]. Nonlinear autoregressive ANN with exogenous inputs was demonstrated in [29] to be superior to nonlinear autoregressive model in the prediction of 1-year hourly wind speed data. Back propagation and support vector machine methods and their hybrids with empirical mode decomposition and wavelet transform, and an ensemble of the methods were used to predict wind speed in [30] and found that ensemble approaches predict better than the individual methods. A method which used analysis of variance to classify wind data into different categories, used stacked de-noising auto-encoder for training the classified data and finally used extreme learning machine to fine-tune and forecast from the trained model was proposed in [31]. Their method predicted better than the adaptive neuron-fuzzy inference system. Other decomposition-based hybrid forecasting methods that are implemented with extreme learning machine were verified experimentally in [32]. In the work [33], a method which first decomposed wind speed data using wavelet technique followed by the modelling of the decomposed wind speed data

sets using recurrent wavelet neural network was seen to out-perform a conventional recurrent neural network. Hybrid methods based on wavelet decomposition and wavelet neural network optimized with Cuckoo search algorithm were used to predict wind speed data collected at two wind farms in China [34]. A novel method which applies echo state network to combine forecasts of several hybrid models was proposed in [35]. A two-part scheme consisting of point prediction based on nonlinear combination and interval prediction based on fuzzy clustering was successfully used to predict wind speed in [36]. Other works on forecasting wind speed time series using artificial intelligence can be found in [37–40].

The reviewed works indicate that successful prediction of wind speed relies on making appropriate choice of filtering, decomposition or classification techniques and applying appropriate modelling approaches to the sub-models. Based on the above review, popular decompositions techniques in wind speed forecasting are empirical mode decomposition, ensemble empirical mode decomposition, fast ensemble empirical mode decomposition, wavelet decomposition, wavelet packet decomposition and their modifications and hybrids. In this work, HPF is applied in decomposing wind speed time series followed by a hybrid use of HA and ML for predicting wind speed from the decomposition components. Hodrick-Prescott Filter is a popular tool in macroeconomics for separating short run fluctuations from long run trend [41] which is innovatively applied in wind speed time series prediction here. The sequential applications of HPF and HA to enhance the accuracy of ML methods for wind speed time series prediction is the major contribution of this work.

Section 2 describes the elements of the proposed methodology including the goodness of fit metrics while Sect. 3 presents the results and discussion which highlight the capacity of the proposed sequential applications of HPF and HA for enhancing the accuracy of ML methods. Section 4 summarizes the conclusions drawn from the study.

2. Methodology

2.1. Hodrick-Prescott Filter

Hodrick-Prescott Filter was developed in macroeconomic analysis for decomposition of observed time series into trend and cyclic parts [42]. The filter is based on minimizing the objective function

$$\sum_{j=1}^J (d_j - \tau_j)^2 + \lambda \sum_{j=2}^{J-1} (\tau_{j+1} - 2\tau_j + \tau_{j-1})^2$$

1
with respect to τ where J is the sample size, λ is the smoothing parameter that has the values 100, 1600 and 14400 for yearly, quarterly and monthly data periodicities. The first sum captures the minimization of the cyclic component while the second sum captures the minimization the second-order difference of the trend component. Hodrick-Prescott Filter is introduced in this work for decomposition of wind speed time series as the first step of seasonality adjustment. At every j -th time step for $j = 1, 2, \dots, J$, HPF decomposes the observation as follows;

$$d_j = d_{j,T} + d_{j,C}$$

2
where $d_{j,T}$ is the trend component and $d_{j,C}$ is the cyclic component. It is known that seasonality compromises the predictive capacity of ANNs in many time series applications [43–45], therefore, the motivation to separate $d_{j,C}$ from the raw data for more treatments.

2.2. Harmonic Analysis

Harmonic analysis is based on the Fourier series of a function that satisfy the Dirichlet conditions. The Fourier series for a periodic function of time is

$$y(t) = \frac{y^{(E.0)}}{2} + \sum_{r=1}^{\infty} \left(y^{(E.r)} \cos r\omega t + y^{(O.r)} \sin r\omega t \right)$$

3

where

$$y^{(E.r)} = \frac{2}{T} \int_{t_0}^{t_0+T} y(t) \cos r\omega t dt$$

4

,

$$y^{(O.r)} = \frac{2}{T} \int_{t_0}^{t_0+T} y(t) \sin r\omega t dt$$

5

,

and $T = 2\pi / \omega$ is the period. The idea here is to consider the cyclic component $d_{j,C}$ from the HPF as a linear combination of a periodic function and a stochastic function. This is conceived to be analogous to considering an experimental measurement of a periodic system to have been compromised by random error. Therefore,

$$d_{j,C} = y_{j,CP} + d_{j,CS}$$

6

where the periodic part $y_{j,CP}$ is then expressed in Fourier series as

$$y_{CP}(t) = \frac{y_{CP}^{(E.0)}}{2} + \sum_{r=1}^{\infty} \left(y_{CP}^{(E.r)} \cos r\omega t + y_{CP}^{(O.r)} \sin r\omega t \right)$$

7

,

$$y_{CP}^{(E.r)} \cong \frac{2}{T} \sum_{j=1}^J C_j y_{j,C} \cos r\omega t_j$$

8

,

$$y_{CP}^{(O.r)} \cong \frac{2}{T} \sum_{j=1}^J C_j y_{j,C} \sin r\omega t_j$$

9

.

Integral quadrature is used to arrive at the forms in Equations (8) and (9) where C_j are coefficients that depend on the limits of integration, number of integration intervals ($J - 1$) and the order or degree of integrand. The Newton-Coates methods are used here for numerical integration. The stochastic component, therefore, becomes

$$d_{j,CS} = d_{j,C} - y_{CP}(t_j)$$

10

The daily and monthly data are considered to have yearly periodicity meaning that t_j is the day or month number for the daily and monthly data, respectively. The seasonality adjusted data (the data resulting from the exclusion of the periodic component from the raw data), given as

$$d_{j,A} = d_{j,T} + d_{j,CS}$$

11

can then be modeled with various ML methods.

2.3. The Anns

Multiple Layer Perceptron (MLP), based on the back-propagation algorithm, is the ANN architecture adopted here. The details of the back-propagation algorithm can be found in [46]. A parallel set of nodes or neurons constitute a layer of an MLP while various layers are connected in series to form a functional MLP network. For example, the following equations hold for the i th node in the p th layer, where $p = 1, 2, \dots, P$, see Fig. 1;

$$n_i^{(p)} = \theta_i^{(p)} + \sum_{k=1}^{I_{p-1}} w_{ki}^{(p)} x_k^{(p)} = \sum_{k=0}^{I_{p-1}} w_{ki}^{(p)} x_k^{(p)}$$

12

$$x_i^{(p)} = g(n_i^{(p)})$$

13

In the equations, the inputs are $x_k^{(p-1)}$ for $k = 1, 2, \dots, I_{p-1}$, the weights are $w_{ki}^{(p)}$, the bias is $\theta_i^{(p)}$, the weighted sum from the summer is $n_i^{(p)}$, the nonlinear activation function is g and the nodal output is $x_i^{(p)}$. As seen in Eq. (12), a compact representation denotes $\theta_i^{(p)}$ as $w_{0i}^{(p)} x_0^{(p)}$ where $w_{0i}^{(p)} = 1$ and $x_0^{(p)} = \theta_i^{(p)}$. In MLP, the nodal outputs of the p th layer are channeled into the nodes of the $(p + 1)$ th layer as inputs, and so on. For example, a single hidden layer network depicted in Fig. 2 (a) (that is, the shallow network with $P = 1$) has the single output

$$y_{j,A} = f(\mathbf{W}g(\mathbf{W}^{(1)}\mathbf{x}_j))$$

14

where the input is $\mathbf{x}_j \in \mathbb{R}^K$, the number of variables in the input layer of the ANN or the lags is K , and the weight matrices are

$$\mathbf{W}^{(1)} = \begin{pmatrix} w_{01}^{(1)} & w_{11}^{(1)} & w_{21}^{(1)} & \cdots & w_{K1}^{(1)} \\ w_{02}^{(1)} & w_{12}^{(1)} & w_{22}^{(1)} & \cdots & w_{K2}^{(1)} \\ \vdots & \vdots & \vdots & \cdots & \vdots \\ w_{0I_1}^{(1)} & w_{1I_1}^{(1)} & w_{2I_1}^{(1)} & \cdots & w_{KI_1}^{(1)} \end{pmatrix}$$

15

,

$$\mathbf{W} = \{ w_{01} \quad w_{11} \quad w_{21} \quad \cdots \quad w_{I_1 1} \}$$

16

.

A two-layer network represented in Fig. 2 (b) (that is the deep network with $P = 2$) has the single output

$$y_{j,A} = f\left(\mathbf{W}g\left(\mathbf{W}^{(2)}g\left(\mathbf{W}^{(1)}\mathbf{x}_j\right)\right)\right)$$

17

where the weight matrix $\mathbf{W}^{(1)}$ is the same as above and

$$\mathbf{W}^{(2)} = \begin{pmatrix} w_{01}^{(2)} & w_{11}^{(2)} & w_{21}^{(2)} & \cdots & w_{I_1 1}^{(2)} \\ w_{02}^{(2)} & w_{12}^{(2)} & w_{22}^{(2)} & \cdots & w_{I_1 2}^{(2)} \\ \vdots & \vdots & \vdots & \cdots & \vdots \\ w_{0I_2}^{(2)} & w_{1I_2}^{(2)} & w_{2I_2}^{(2)} & \cdots & w_{I_1 I_2}^{(2)} \end{pmatrix}$$

18

,

$$\mathbf{W} = \{ w_{01} \quad w_{11} \quad w_{21} \quad \cdots \quad w_{I_2 1} \}$$

19

.

The sum of the errors

$$\epsilon_{\text{tot}} = \frac{1}{2} \sum_j (y_{j,A} - d_{j,A})^2$$

20

,

where $d_{j,A}$ is the target at the j -th time step, is minimized in terms of the weight parameters $w_{ki}^{(p)}$ and w_{ki} using a weights-adjustment algorithm that is initiated with a numerical choice of the weight matrices. A properly specified learning rate η is used to increment the weight parameters the q -th iteration for the $(q + 1)$ -th iteration as follows

$$w_{ki}^{(p)}(q+1) = w_{ki}^{(p)}(q) - \eta \frac{\partial e_{\text{tot}}}{\partial w_{ki}^{(p)}}(q)$$

21

The iterations are implemented using the chain rule and backpropagation algorithm [46]. Levenberg-Marquardt algorithm, as adopted in this work, is typically used to teach MLPs. Here, the functions g and f are based on tangent sigmoid (tansig) and linear (purelin) transfer functions respectively.

2.4. Regression-Based ML Methods

Multiple linear regression models are calibrated from the matrix equation

$$\mathbf{d} = \mathbf{X} \mathbf{\varvec{\beta}} + \mathbf{E}$$

22

where, for the current application, $\mathbf{d} = \{d_{1,A} \ d_{2,A} \ \dots \ d_{J,A}\}^T$ is the vector of the seasonality adjusted target wind speed, $\mathbf{X} \in \mathbb{R}^{J \times K}$ is the matrix of the seasonality adjusted delayed predictor wind speeds, $\mathbf{\varvec{\beta}} = \{\beta_1 \ \beta_2 \ \dots \ \beta_K\}^T$ is the vector of model coefficients, $\mathbf{E} \in \mathbb{R}^{J \times 1}$ is a vector of randomly distributed error. Being a parametric method, multiple linear regression considers the elements of $\mathbf{\varvec{\beta}}$ as fixed coefficients of polynomials to be calibrated using the least squares method. Therefore,

$$\mathbf{\varvec{\beta}} = \{\mathbf{X}^T \mathbf{X}\}^{-1} \mathbf{X}^T \mathbf{d}$$

23

The calibrated model becomes

$$y_A = \mathbf{x}^T \mathbf{\varvec{\beta}}$$

24

where \mathbf{x} is the row of variables representing the seasonality adjusted delayed predictor wind speeds including a unit value which represent the intercept.

The support vector machine and Gaussian process regressions are non-parametric methods that rely on kernel functions. For the linear support vector machines, the regression model is constructed as

$$y_A = \mathbf{x}^T \mathbf{\varvec{\beta}} + \beta_0$$

25

where $\mathbf{\varvec{\beta}}$ parameter is expressed as a linear combination of the input patterns \mathbf{x}_{ij} leading to

$$y_{\text{A}} = \sum_{j=1}^J \left(\alpha_n - \alpha_n^{\text{bf}^*} \right) \mathbf{x}_{\text{T}}^j + \beta_0$$

26

The input patterns are support vectors when either of the two Lagrange multipliers α_n and $\alpha_n^{\text{bf}^*}$ is non zero. The parameters α_n , $\alpha_n^{\text{bf}^*}$ and β_0 are calibrated by optimizing the objective function

$$E(\vec{\beta}) = \frac{1}{2} \vec{\beta}^T \mathbf{v} \mathbf{v}^T \vec{\beta}$$

27

where

$$\vec{\beta} = \sum_{j=1}^J \left(\alpha_n - \alpha_n^{\text{bf}^*} \right) \mathbf{x}_{\text{T}}^j$$

28

subject to the Karush-Kuhn-Tucker constraints [47]. The Gaussian process regression is a Bayesian method based on the model of form

$$y_{\text{A}} = \mathbf{x}_{\text{T}}^T \vec{\beta} + \epsilon$$

29

where ϵ is normally distributed error with zero mean and fixed variance σ^2 and $\vec{\beta}$ is a vector of basis function coefficients. To explain the response in Gaussian process regression, the latent variables \mathbf{x}_{T}^j are introduced for $j = 1, 2, \dots, J$ to form a Gaussian process. The details on Gaussian process regression can be found [48]. In addition to the above-described regression methods, fine regression trees and boosted ensembles of trees as available in MatLab are also used for illustration in this work.

2.5. Goodness of Fit Indices

The accuracy of the models are assessed and compared using the following goodness of fit (GOF) indices; the coefficient of determination R^2 , root mean square error (RMSE), bias (MBE), absolute bias (MABE), mean percentage error (MPE), and correlation coefficient (CC). They are expressed as follows;

$$R^2 = 1 - \frac{\sum_{j=1}^J (d_j - y_j)^2}{\sum_{j=1}^J (d_j - \bar{y})^2}$$

30

root mean square error (RMSE) which is given as

$$R_{\text{MSE}} = \sqrt{\frac{1}{\sum_{j=1}^J} \sum_{j=1}^J (y_j - d_j)^2}$$

31

mean bias error (MBE) which is given as

$$M_{\text{BE}} = \frac{1}{\sum_{j=1}^J} \sum_{j=1}^J (y_j - d_j)$$

32

mean absolute bias error (MABE) which is given as

$$\text{MABE} = \frac{1}{\sum_{j=1}^n} \sum_{j=1}^n \left| \frac{y_j - d_j}{d_j} \right|$$

mean percentage error (MPE) which is given as

$$\text{MPE} = \frac{1}{\sum_{j=1}^n} \sum_{j=1}^n \left(\frac{y_j - d_j}{d_j} \right) \times 100$$

and correlation coefficient (r) which is given as

$$r = \frac{\sum_{j=1}^n (y_j - \bar{y})(d_j - \bar{d})}{\sqrt{\sum_{j=1}^n (y_j - \bar{y})^2 \sum_{j=1}^n (d_j - \bar{d})^2}}$$

where $y_j = y_j, \text{A} + y_j, \text{C} + y_j, \text{P}$ and $d_j = d_j, \text{A} + d_j, \text{C} + d_j, \text{P}$.

2.6. The Analytical Procedure

The proposed analytical procedure is illustrated in Fig. 3. Firstly, the raw wind speed data is decomposed into trend $\{d_j, \text{T}\}$ and cyclic $\{d_j, \text{C}\}$ components using the MatLab command for HPF. Secondly, the periodic sub-component $\{y_j, \text{C}\} = \{y_j, \text{C}\} \left(\frac{t}{T} \right)$ is extracted from the cyclic component $\{d_j, \text{C}\}$ using HA based on numerical integration, and the stochastic sub-component $\{d_j, \text{C}\} \text{S}$ is then calculated as the difference $\{d_j, \text{C}\} - \{y_j, \text{C}\}$. The sums $\{d_j, \text{C}\} \text{S} + \{d_j, \text{T}\}$ serve as the adjusted wind speeds $\{d_j, \text{A}\}$. For $j=K, K+1 \dots J$, the input vector of delayed time series $\{\mathbf{x}_j\} = \left(\begin{array}{c} d_{j-K}, \text{A} \\ d_{j-K+1}, \text{A} \\ \dots \\ d_{j-1}, \text{A} \end{array} \right)^{\text{T}}$ are formed to serve as the input to ML methods for making the predictions $\{y_j, \text{A}\}$. The exploited ML methods are implemented in codes adapted from MatLab tools. The predicted wind speeds are finally calculated as the sums $y_j = y_j, \text{A} + y_j, \text{C} + y_j, \text{P}$.

3. Results And Discussion

Daily and monthly mean wind speed data for Enugu (6.470°N, 7.550°E) in Nigeria and Stuttgart (48.782°N, 9.174°E) in Germany were gotten from the website of Modern-Era Retrospective Analysis for Research and Applications, Version 2 (MERRA-2). The collected wind speed data for the height of 10m above ground level run from January 1980 to June 2020.

The current wind speed is dependent on four wind speed lags for the monthly data while it is dependent on six or five wind speed lags for the daily data, see the correlograms in Figs. 4 and 5. For the monthly data, the correlations of yearly lags seem to be significant but the correlations are small relative to the first four monthly lags, therefore, are ignored. Four and five lags are, therefore, used for monthly and daily models, respectively. The graphs of the prediction results are shown in Figs. 6 to 9 while the GOF indices are summarized in Tables 1 to 8. The first part of each of Figs. 6 to 9 shows the results of all the ML methods enhanced with HPF and HA pretreatments. The results of the enhanced methods are indicated by prefixing the acronym of the ML methods with "HPF-HA-" while the results of the

corresponding non-enhanced methods are shown in the adjacent figures without the prefix. In addition to the endogenous lags, the inputs to the non-enhanced ML methods includes the exogenous time parameter (month or day number). This is necessary for fair comparisons since time parameter is introduced in the enhanced methods via the HA, and also necessary for assessing the influence of seasonality on predictive accuracy of the ML methods. A comparative look on the two components of each of the figures shows that the proposed wind speed prediction procedure considerably improves accuracy relative to the non-enhanced methods. The GOF indices in Tables 1, 3, 5 and 7 for the proposed methods show high correlations (R^2 and CC) and low errors (RMSE, MBE, MABE, MPE) between the predicted and target data, and show that the indices for the testing and training are comparable meaning that the trained models can be used for predicting from independent data. This is not the case for the non-enhanced ML methods as seen in Tables 2, 4, 6 and 8 which show significantly lower correlations and higher errors, and show significantly devalued indices for testing compared to training meaning that the trained models cannot be reliably used for predicting from independent data. The improvement is visible in the figures as less horizontal scatter which indicates the significant better capacity of the enhanced ML methods to model the variation in the target data. This means that the presence of seasonality in the raw data weakens the predictive capacity of the non-enhanced methods.

In terms of the performance index MPE, the enhancement ANN with HPF and HA reduced the training error from 23.04–1.06% for monthly prediction for Enugu, and from 35.79–2.06% for Stuttgart. For daily prediction, the error reductions are from 23.62–11.23% and 55.71–6.77% for Enugu and Stuttgart, respectively. Under testing, the improvements are 38.85–1.98% and 27.20% to 10.49 % for monthly and daily predictions of Enugu wind speed while the improvements are respectively 44.85–2.15% and 46.80–6.81% for Stuttgart. Similar scales of improvements are seen for the other ML methods by comparing the corresponding values in the tables of GOF indices. The need to watch against over-fitting arises with the use of BET (and FRT to a lesser degree) especially in the prediction of daily wind speed. This can be seen in Tables 1, 3, 5 and 7 as more pronounced devaluation of the GOF indices (see R^2 for example) of testing compared to training than can be seen for the other ML methods.

Table 1
The goodness of fit indices of monthly wind speed predictions with HPF and HA pretreatments for Enugu

Lat. [° N]	6.470											
Long. [° E]	7.550											
Model	HPF-HA-ANN		HPF-HA-LRI		HPF-HA-SVM		HPF-HA-RQGPR		HPF-HA-FRT		HPF-HA-BET	
	Train	Test	Train	Test	Train	Test	Train	Test	Train	Test	Train	Test
R^2	0.97	0.94	0.95	0.95	0.95	0.94	0.95	0.95	0.98	0.93	1.00	0.91
RMSE	0.12	0.17	0.15	0.16	0.16	0.16	0.15	0.16	0.11	0.18	0.00	0.21
MBE	-0.00	-0.00	-0.00	0.00	-0.00	0.00	0.00	0.01	-0.00	-0.01	-0.00	-0.00
MABE	0.09	0.14	0.12	0.12	0.12	0.12	0.11	0.12	0.08	0.14	0.00	0.16
MPE	1.06	1.98	1.85	2.87	1.89	2.80	1.70	2.89	0.83	1.26	0.00	1.96
CC	0.98	0.97	0.98	0.98	0.98	0.98	0.98	0.98	0.99	0.97	1.00	0.95

Table 2

The goodness of fit indices of monthly wind speed predictions without HPF and HA pretreatments for Enugu

Lat. [° N]	6.470											
Long. [° E]	7.550											
Model	ANN		LRI		SVM		RQGPR		FRT		BET	
	Train	Test	Train	Test	Train	Test	Train	Test	Train	Test	Train	Test
R ²	0.68	0.23	0.38	0.34	0.27	0.35	0.77	0.42	0.74	0.20	1.00	-0.00
RMSE	0.51	0.78	0.71	0.72	0.78	0.72	0.43	0.68	0.46	0.80	0.01	0.89
MBE	-0.00	0.03	-0.00	-0.00	0.05	0.04	0.00	0.05	-0.00	0.02	-0.00	0.01
MABE	0.38	0.55	0.54	0.55	0.58	0.55	0.33	0.47	0.31	0.59	0.00	0.66
MPE	23.04	38.85	47.87	37.96	56.22	40.52	25.87	34.73	22.10	31.66	0.01	32.32
CC	0.83	0.56	0.62	0.59	0.53	0.59	0.89	0.66	0.86	0.57	1.00	0.51

Table 3

The goodness of fit indices of monthly wind speed predictions with HPF and HA pretreatments for Stuttgart

Lat. [° N]	48.782											
Long. [° E]	9.174											
Model	HPF-HA-ANN		HPF-HA-LRI		HPF-HA-SVM		HPF-HA-RQGPR		HPF-HA-FRT		HPF-HA-BET	
	Train	Test	Train	Test	Train	Test	Train	Test	Train	Test	Train	Test
R ²	0.88	0.86	0.84	0.86	0.84	0.86	0.84	0.86	0.92	0.74	1.00	0.72
RMSE	0.19	0.24	0.22	0.23	0.23	0.23	0.22	0.23	0.16	0.31	0.00	0.32
MBE	-0.00	-0.00	-0.00	-0.04	-0.01	-0.04	-0.00	-0.04	-0.00	-0.06	-0.00	-0.00
MABE	0.15	0.17	0.18	0.18	0.18	0.19	0.18	0.18	0.12	0.24	0.00	0.25
MPE	2.06	2.15	2.75	0.59	2.18	0.30	2.69	0.47	1.41	0.30	0.00	2.63
CC	0.94	0.93	0.92	0.94	0.92	0.93	0.92	0.94	0.96	0.87	1.00	0.85

Table 4

The goodness of fit indices of monthly wind speed predictions without HPF and HA pretreatments for Stuttgart

Lat. [° N]	48.782											
Long. [° E]	9.174											
Model	ANN		LRI		SVM		RQGPR		FRT		BET	
	Train	Test	Train	Test	Train	Test	Train	Test	Train	Test	Train	Test
R ²	0.42	-0.55	0.09	0.02	0.02	0.02	0.15	0.02	0.57	-0.78	1.00	-0.99
RMSE	0.82	1.05	1.03	1.07	0.83	0.83	1.00	0.83	0.71	1.12	0.01	1.19
MBE	-0.00	0.11	0.00	-0.21	-0.17	-0.17	-0.00	0.03	-0.00	-0.04	0.00	0.03
MABE	0.62	0.79	0.80	0.78	0.64	0.64	0.78	0.64	0.51	0.88	0.01	0.93
MPE	35.79	44.85	60.84	41.72	26.13	26.13	60.16	43.72	24.94	32.60	0.08	31.27
CC	0.65	0.12	0.31	0.24	0.25	0.25	0.43	0.18	0.75	0.01	1.00	0.16

Table 5

The goodness of fit indices of daily wind speed predictions with HPF and HA pretreatments for Enugu

Lat. [° N]	6.470											
Long. [° E]	7.550											
Model	HPF-HA-ANN		HPF-HA-LRI		HPF-HA-SVM		HPF-HA-RQGPR		HPF-HA-FRT		HPF-HA-BET	
	Train	Test	Train	Test	Train	Test	Train	Test	Train	Test	Train	Test
R ²	0.67	0.68	0.79	0.79	0.79	0.79	0.79	0.79	0.91	0.67	0.87	0.72
RMSE	0.43	0.41	0.34	0.33	0.34	0.33	0.34	0.33	0.22	0.41	0.27	0.38
MBE	0.12	0.12	-0.00	-0.00	0.01	0.01	-0.00	-0.00	0.00	-0.01	0.00	-0.00
MABE	0.33	0.32	0.26	0.25	0.26	0.25	0.26	0.25	0.17	0.32	0.21	0.29
MPE	11.23	10.49	2.75	2.21	2.84	2.28	2.75	2.21	1.19	2.13	1.74	2.18
CC	0.85	0.86	0.89	0.89	0.89	0.89	0.89	0.89	0.96	0.83	0.93	0.85

Table 6

The goodness of fit indices of daily wind speed predictions without HPF and HA pretreatments for Enugu

Lat. [° N]	6.470											
Long. [° E]	7.550											
Model	HPF-HA-ANN		HPF-HA-LRI		HPF-HA-SVM		HPF-HA-RQGPR		HPF-HA-FRT		HPF-HA-BET	
	Train	Test	Train	Test	Train	Test	Train	Test	Train	Test	Train	Test
R ²	0.53	0.52	0.51	0.51	0.51	0.50	0.51	0.51	0.81	0.24	0.69	0.39
RMSE	0.70	0.71	0.71	0.72	0.71	0.72	0.71	0.72	0.45	0.89	0.57	0.80
MBE	-0.00	0.01	-0.00	0.02	0.02	0.04	0.00	0.02	0.00	0.02	-0.00	0.01
MABE	0.55	0.56	0.56	0.57	0.56	0.57	0.56	0.57	0.34	0.71	0.44	0.63
MPE	23.62	27.20	23.99	27.69	24.17	27.94	24.11	27.89	10.24	28.48	15.01	27.23
CC	0.73	0.72	0.72	0.71	0.72	0.71	0.72	0.71	0.90	0.58	0.83	0.65

Table 7

The goodness of fit indices of daily wind speed predictions with HPF and HA pretreatments for Stuttgart

Lat. [° N]	48.782											
Long. [° E]	9.174											
Model	HPF-HA-ANN		HPF-HA-LRI		HPF-HA-SVM		HPF-HA-RQGPR		HPF-HA-FRT		HPF-HA-BET	
	Train	Test	Train	Test	Train	Test	Train	Test	Train	Test	Train	Test
R ²	0.62	0.59	0.63	0.60	0.61	0.59	0.63	0.61	0.83	0.40	0.76	0.49
RMSE	0.63	0.65	0.62	0.64	0.63	0.65	0.61	0.63	0.41	0.78	0.50	0.72
MBE	0.10	0.10	0.00	0.00	-0.10	-0.10	-0.00	0.00	0.00	-0.00	0.00	0.00
MABE	0.50	0.51	0.47	0.49	0.47	0.48	0.47	0.48	0.30	0.60	0.38	0.55
MPE	6.77	6.81	3.28	3.36	0.12	0.17	3.28	3.36	1.42	3.34	2.34	3.33
CC	0.79	0.78	0.79	0.77	0.79	0.78	0.79	0.78	0.91	0.67	0.87	0.71

Table 8

The goodness of fit indices of daily wind speed predictions without HPF and HA pretreatments for Stuttgart

Lat. [° N]	48.782											
Long. [° E]	9.174											
Model	HPF-HA-ANN		HPF-HA-LRI		HPF-HA-SVM		HPF-HA-RQGPR		HPF-HA-FRT		HPF-HA-BET	
	Train	Test	Train	Test	Train	Test	Train	Test	Train	Test	Train	Test
R ²	0.28	0.26	0.29	0.27	0.29	0.27	0.31	0.28	0.71	-0.14	0.57	0.06
RMSE	1.57	1.56	1.56	1.55	1.57	1.56	1.54	1.54	0.99	1.95	1.22	1.77
MBE	0.17	0.11	0.00	-0.06	-0.12	-0.18	-0.00	-0.06	0.00	-0.06	0.00	-0.05
MABE	1.23	1.22	1.21	1.20	1.21	1.20	1.19	1.19	0.75	1.51	0.96	1.35
MPE	55.71	46.80	46.37	37.70	40.61	32.16	46.26	37.82	19.73	39.36	34.33	37.44
CC	0.54	0.52	0.54	0.52	0.54	0.53	0.56	0.53	0.84	0.34	0.75	0.41

4. Conclusions

In this work, the capacities of various machine learning methods for time series modelling and forecasting of daily and monthly wind speed are enhanced by introducing two-step filtration of the target data using HPF and HA, in that order. The key results are itemized as follows:

Predictive accuracy is improved when the following four analytical steps are integrated in the so-called enhanced ML methods. Firstly, the raw wind speed data is decomposed into trend and cyclic components using HPF. Secondly, the cyclic component is decomposed into the periodic and stochastic sub-components using HA. Thirdly, ML methods are applied in modelling the sum of the trend and stochastic time series. Finally, wind speed predictions are integrated from the outputs of ML methods and harmonic analyses.

Compared to the non-enhanced ML methods which are applied directly on the raw data, the enhanced ML methods are found to have markedly improved prediction accuracy of daily and monthly wind speed time series. For example, mean percentage error typically reduced from 44.85% to 2.15% and 46.80% to 6.81% for monthly and daily predictions on testing the ANN-trained models. The poor performance of the non-enhanced ML methods is as a result of the effects of seasonality in the raw data.

Amongst the six ML methods adopted for illustrative purposes, ANN, LRI, SVM, RQGPR are recommended because of the high predictive accuracy of the trained models from new data while the tree-based methods (BET and FRT) are not recommended because of overfitting issues.

5. Abbreviations

Symbol	Name
ANN	artificial neural networks
BETs	boosted ensembles of trees
$\{d\}_{-j}$	target wind speed
FRTs	fine regression trees
GOF	goodness of fit
HPF	Hodrick-Prescott Filter
$\{l\}_{-p}$	number of neurons in thepth hidden layer of an ANN
K	lags in an input vector
MABE	mean absolute bias error
MBE	mean bias error
MERRA-2	Modern-Era Retrospective analysis for Research and Applications, Version 2
ML	machine learning
MLP	multi-layer perceptron
MPE	mean percentage error
η	is the learning rate of ANN
J	number of time steps in the training or testing sets
P	no of hidden layers in MLP ANN
CC	correlation coefficient
RMSE	root mean square error
R^2	coefficient of determination
RQGPR	rational quadratic Gaussian process regression
SVM	support vector machine
$\{\mathbf{x}\}_{-j}$	input vectors
$\{y\}_{-j}$	predicted wind speed

6. Declarations

Funding (Comdalytics Nigeria Limited provided financial support (Grant ID:2021001) for this research. This funding is highly appreciated)

Conflicts of interest/Competing interests (Not applicable)

Availability of data and material (Not applicable)

Code availability (custom code available)

7. References

- [1] Savino JM. Wind power. vol. 22. 1975. doi:10.1049/ep.1976.0231.
- [2] Kaldellis JK, Zafirakis D. The wind energy (r)evolution: A short review of a long history. *Renew Energy* 2011;36:1887–901. doi:10.1016/j.renene.2011.01.002.
- [3] Petersen EL. In search of the wind energy potential. *J Renew Sustain Energy* 2017;9. doi:10.1063/1.4999514.
- [4] Bradford T. Solar revolution: the economic transformation of the global energy industry. vol. 32. 2006. doi:10.1016/j.energy.2007.03.002.
- [5] Keivanpour S, Ramudhin A, Ait Kadi D. The sustainable worldwide offshore wind energy potential: A systematic review. *J Renew Sustain Energy* 2017;9. doi:10.1063/1.5009948.
- [6] Sahin AD. Progress and recent trends in wind energy. *Prog Energy Combust Sci* 2004;30:501–43. doi:10.1016/j.pecs.2004.04.001.
- [7] REN21. Renewables 2017: Global status report. Paris: 2017. doi:10.1016/j.rser.2016.09.082.
- [8] Fadare DA. The application of artificial neural networks to mapping of wind speed profile for energy application in Nigeria. *Appl Energy* 2010;87:934–42. doi:10.1016/j.apenergy.2009.09.005.
- [9] Barati H, Haroonabadi H, Zadehali R. Wind speed forecasting in South Coasts of Iran: An Application of Artificial Neural Networks (ANNs) for Electricity Generation using Renewable Energy. *Bull Environ Pharmacol Life Sci* 2013;2:30–7.
- [10] Brahim T. Using artificial intelligence to predict wind speed for energy application in Saudi Arabia. *Energies* 2019;12. doi:10.3390/en12244669.
- [11] Liu H, Tian HQ, Pan DF, Li YF. Forecasting models for wind speed using wavelet, wavelet packet, time series and Artificial Neural Networks. *Appl Energy* 2013;107:191–208. doi:10.1016/j.apenergy.2013.02.002.
- [12] Arjun NN, Prema V, Kumar DK, Prashanth P, Preekshit VS, Rao KU. Multivariate regression models for prediction of wind speed. *Proc. - 2014 Int. Conf. Data Sci. Eng. ICDSE 2014, 2014*, p. 171–6. doi:10.1109/ICDSE.2014.6974632.
- [13] Barhmi S, Elfatni O, Belhaj I. Forecasting of wind speed using multiple linear regression and artificial neural networks. *Energy Syst* 2019. doi:10.1007/s12667-019-00338-y.
- [14] Li G, Shi J. On comparing three artificial neural networks for wind speed forecasting. *Appl Energy* 2010;87:2313–20. doi:10.1016/j.apenergy.2009.12.013.
- [15] Chen X, Zhao J, Hu W, Yang Y. Short-term wind speed forecasting using decomposition-based neural networks combining abnormal detection method. *Abstr Appl Anal* 2014;2014. doi:10.1155/2014/984268.
- [16] Santhosh M, Venkaiah C, Vinod Kumar DM. Ensemble empirical mode decomposition based adaptive wavelet neural network method for wind speed prediction. *Energy Convers Manag* 2018;168:482–93. doi:10.1016/j.enconman.2018.04.099.

- [17] Liu H, Tian HQ, Liang XF, Li YF. Wind speed forecasting approach using secondary decomposition algorithm and Elman neural networks. *Appl Energy* 2015;157:183–94. doi:10.1016/j.apenergy.2015.08.014.
- [18] Liu H, Tian HQ, Li YF. Four wind speed multi-step forecasting models using extreme learning machines and signal decomposing algorithms. *Energy Convers Manag* 2015;100:16–22. doi:10.1016/j.enconman.2015.04.057.
- [19] Sun N, Zhou J, Liu G, He Z. A hybrid wind speed forecasting model based on a decomposition method and an improved regularized extreme learning machine. *Energy Procedia* 2019;158:217–22. doi:10.1016/j.egypro.2019.01.079.
- [20] Liu Y, Zhang S, Chen X, Wang J. Artificial combined model based on hybrid nonlinear neural network models and statistics linear models-research and application for wind speed forecasting. *Sustain* 2018;10. doi:10.3390/su10124601.
- [21] Cai H, Jia X, Feng J, Yang Q, Hsu YM, Chen Y, et al. A combined filtering strategy for short term and long term wind speed prediction with improved accuracy. *Renew Energy* 2019;136:1082–90. doi:10.1016/j.renene.2018.09.080.
- [22] Gendeel M, Yuxian Z, Aoqi H. Performance comparison of ANNs model with VMD for short-term wind speed forecasting. *IET Renew Power Gener* 2018;12:1424–30. doi:10.1049/iet-rpg.2018.5203.
- [23] Guo Z, Zhao W, Lu H, Wang J. Multi-step forecasting for wind speed using a modified EMD-based artificial neural network model. *Renew Energy* 2012;37:241–9. doi:10.1016/j.renene.2011.06.023.
- [24] Liu H, Chen C, Tian HQ, Li YF. A hybrid model for wind speed prediction using empirical mode decomposition and artificial neural networks. *Renew Energy* 2012;48:545–56. doi:10.1016/j.renene.2012.06.012.
- [25] Peng T, Zhou J, Zhang C, Zheng Y. Multi-step ahead wind speed forecasting using a hybrid model based on two-stage decomposition technique and AdaBoost-extreme learning machine. *Energy Convers Manag* 2017;153:589–602. doi:10.1016/j.enconman.2017.10.021.
- [26] Wang L, Li X, Bai Y. Short-term wind speed prediction using an extreme learning machine model with error correction. *Energy Convers Manag* 2018;162:239–50. doi:10.1016/j.enconman.2018.02.015.
- [27] Liu H, Mi X, Li Y. Comparison of two new intelligent wind speed forecasting approaches based on Wavelet Packet Decomposition, Complete Ensemble Empirical Mode Decomposition with Adaptive Noise and Artificial Neural Networks. *Energy Convers Manag* 2018;155:188–200. doi:10.1016/j.enconman.2017.10.085.
- [28] Qu Z, Mao W, Zhang K, Zhang W, Li Z. Multi-step wind speed forecasting based on a hybrid decomposition technique and an improved back-propagation neural network. *Renew Energy* 2019;133:919–29. doi:10.1016/j.renene.2018.10.043.
- [29] Blanchard T, Samanta B. Wind speed forecasting using neural networks. *Wind Eng* 2020;44:33–48. doi:10.1177/0309524X19849846.
- [30] Yong B, Qiao F, Wang C, Shen J, Wei Y, Zhou Q. Ensemble Neural Network Method for Wind Speed Forecasting. *IEEE Work Signal Process Syst SiPS Des Implement* 2019;2019-Octob:31–6. doi:10.1109/SiPS47522.2019.9020410.
- [31] Chen L, Li Z, Zhang Y. Multiperiod-Ahead Wind Speed Forecasting Using Deep Neural Architecture and Ensemble Learning. *Math Probl Eng* 2019;2019. doi:10.1155/2019/9240317.

- [32] Liu H, Mi X, Li Y. An experimental investigation of three new hybrid wind speed forecasting models using multi-decomposing strategy and ELM algorithm. *Renew Energy* 2018;123:694–705. doi:10.1016/j.renene.2018.02.092.
- [33] Pradhan PP, Subudhi B. Wind speed forecasting based on wavelet transformation and recurrent neural network. *Int J Numer Model Electron Networks, Devices Fields* 2020;33:1–11. doi:10.1002/jnm.2670.
- [34] Zhang Y, Yang S, Guo Z, Guo Y, Zhao J. Wind speed forecasting based on wavelet decomposition and wavelet neural networks optimized by the Cuckoo search algorithm. *Atmos Ocean Sci Lett* 2019;12:107–15. doi:10.1080/16742834.2019.1569455.
- [35] Chen Y, He Z, Shang Z, Li C, Li L, Xu M. A novel combined model based on echo state network for multi-step ahead wind speed forecasting: A case study of NREL. *Energy Convers Manag* 2019;179:13–29. doi:10.1016/j.enconman.2018.10.068.
- [36] Nie Y, Bo H, Zhang W, Zhang H. Research on Hybrid Wind Speed Prediction System Based on Artificial Intelligence and Double Prediction Scheme. *Complexity* 2020;2020. doi:10.1155/2020/9601763.
- [37] Foley AM, Leahy PG, Marvuglia A, McKeogh EJ. Current methods and advances in forecasting of wind power generation. *Renew Energy* 2012;37:1–8. doi:10.1016/j.renene.2011.05.033.
- [38] Chang W-Y. A Literature Review of Wind Forecasting Methods. *J Power Energy Eng* 2014;02:161–8. doi:10.4236/jpee.2014.24023.
- [39] Ata R. Artificial neural networks applications in wind energy systems: a review. *Renew Sustain Energy Rev* 2015;49:534–62. doi:10.1016/j.rser.2015.04.166.
- [40] Wang Y, Yu Y, Cao S, Zhang X, Gao S. A review of applications of artificial intelligent algorithms in wind farms. *Artif Intell Rev* 2020;53:3447–500. doi:10.1007/s10462-019-09768-7.
- [41] de Jong R, Sakarya N. The Econometrics of the Hodrick-Prescott filter. *Rev Econ Stat* 2015;92. doi:https://doi.org/10.1162/REST_a_00523.
- [42] Hodrick RJ, Prescott EC. Postwar U.S. Business Cycles: An Empirical Investigation. *J Money, Credit Bank* 1997;29:1. doi:10.2307/2953682.
- [43] Zhang GP, Qi M. Neural network forecasting for seasonal and trend time series. *Eur J Oper Res* 2005;160:501–14. doi:10.1016/j.ejor.2003.08.037.
- [44] Crone SF, Dhawan R. Forecasting seasonal time series with neural networks: A sensitivity analysis of architecture parameters. *IEEE Int. Conf. Neural Networks - Conf. Proc., Orlando, Florida, USA: 2007*, p. 2099–104. doi:10.1109/IJCNN.2007.4371282.
- [45] Claveria O, Monte E, Torra S. Effects of removing the trend and the seasonal component on the forecasting performance of artificial neural network techniques. 2015.
- [46] Haykin S. *Neural networks-A comprehensive foundation*. New York IEEE Press Herrmann, M, Bauer, H-U, Der, R 1994;psychology:pp107-116. doi:10.1017/S0269888998214044.
- [47] Vapnik V. *The Nature of Statistical Learning Theory*. Second. New York: Springer, 2000. doi:10.1007/978-1-4757-2440-0.

Figures

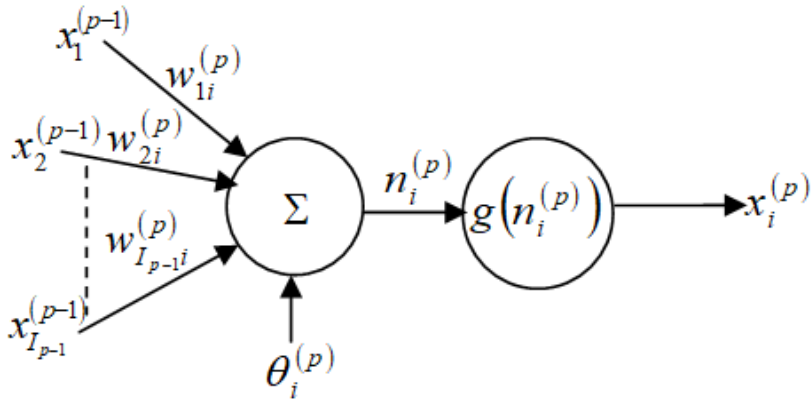


Figure 1

The i th node in the p th layer of an MLP ANN

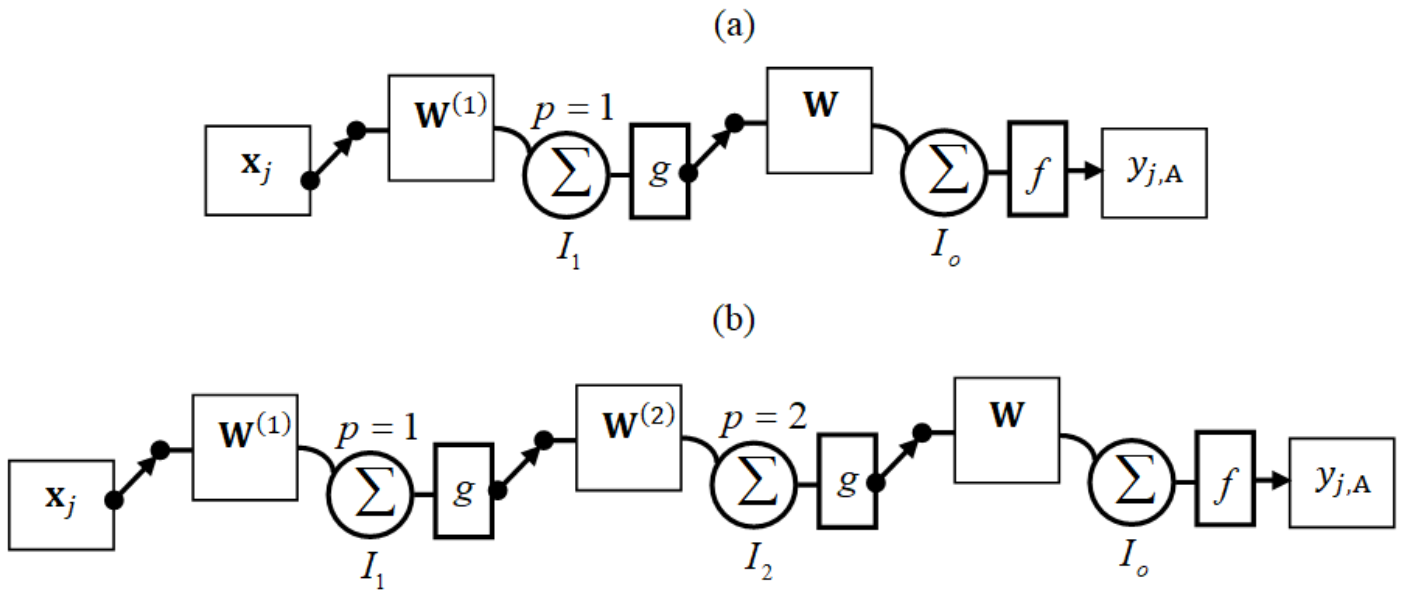


Figure 2

The MLP ANNs with (a) a single hidden layer (b) two hidden layers

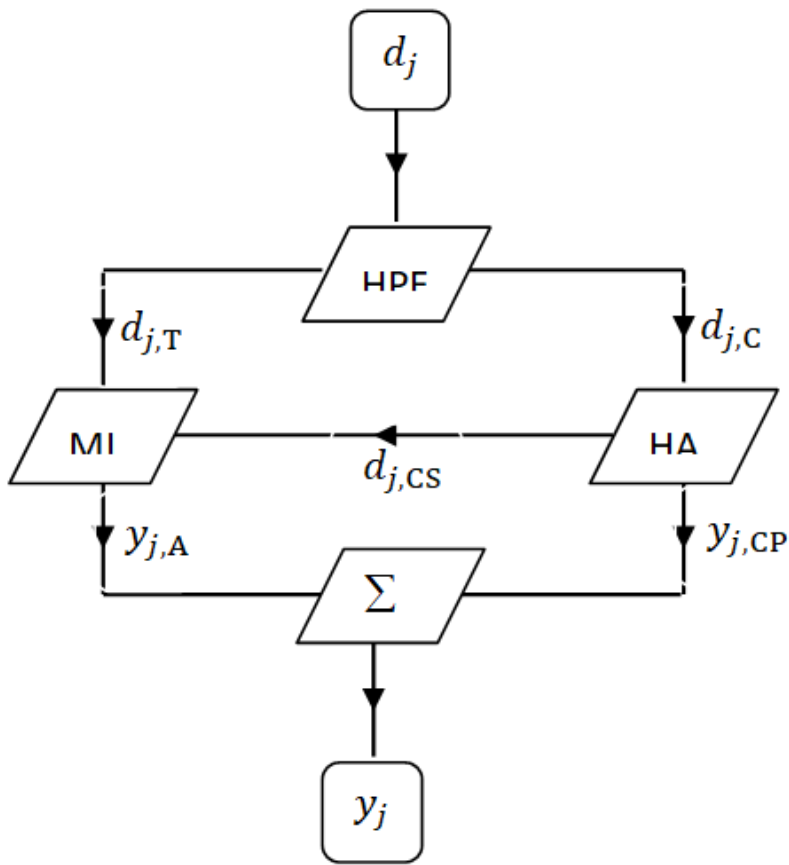


Figure 3

The proposed wind speed prediction procedure.

(a)

(b)

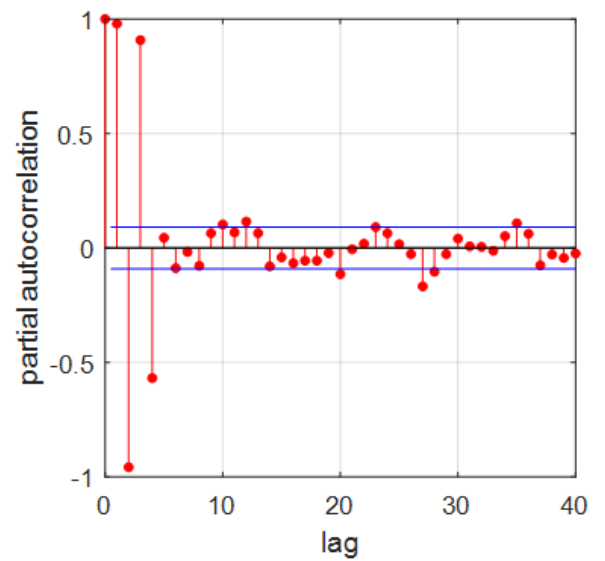
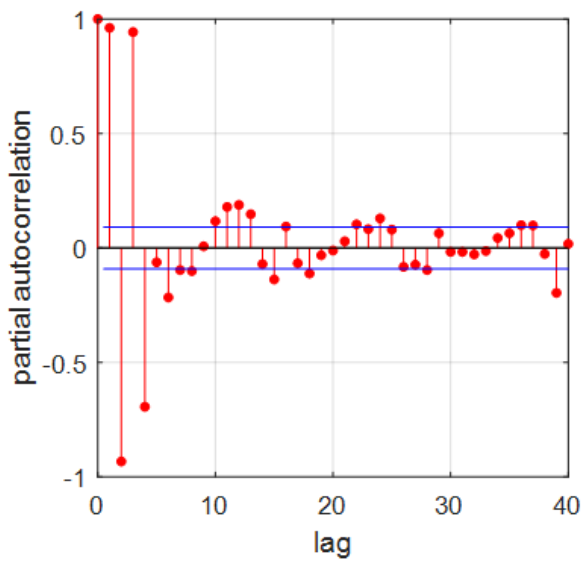


Figure 4

Partial autocorrelation function of monthly wind speed (a) Enugu (b) Stuttgart

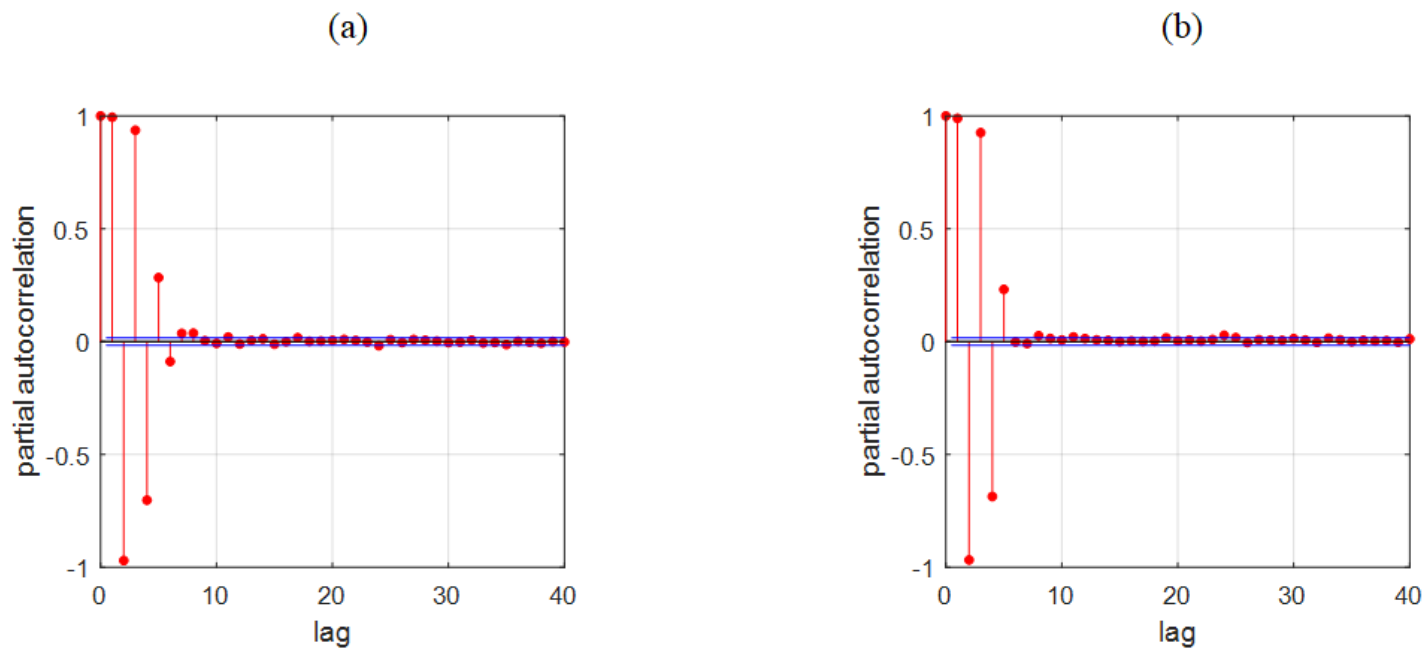


Figure 5

Partial autocorrelation function of daily wind speed (a) Enugu (b) Stuttgart

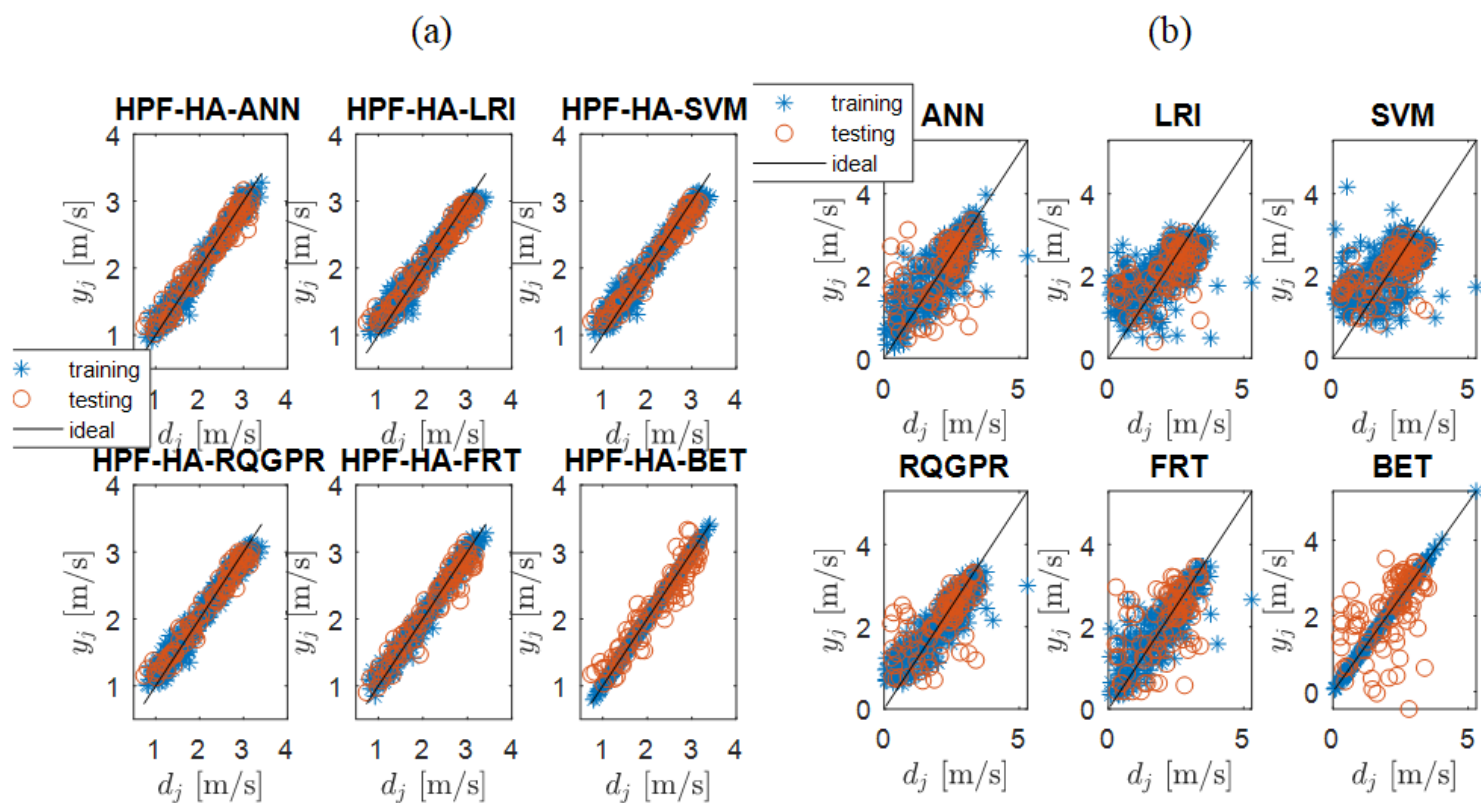


Figure 6

Plots of monthly wind speed predictions for Enugu (a) with HPF and HA pretreatments (b) without HPF and HA pretreatments

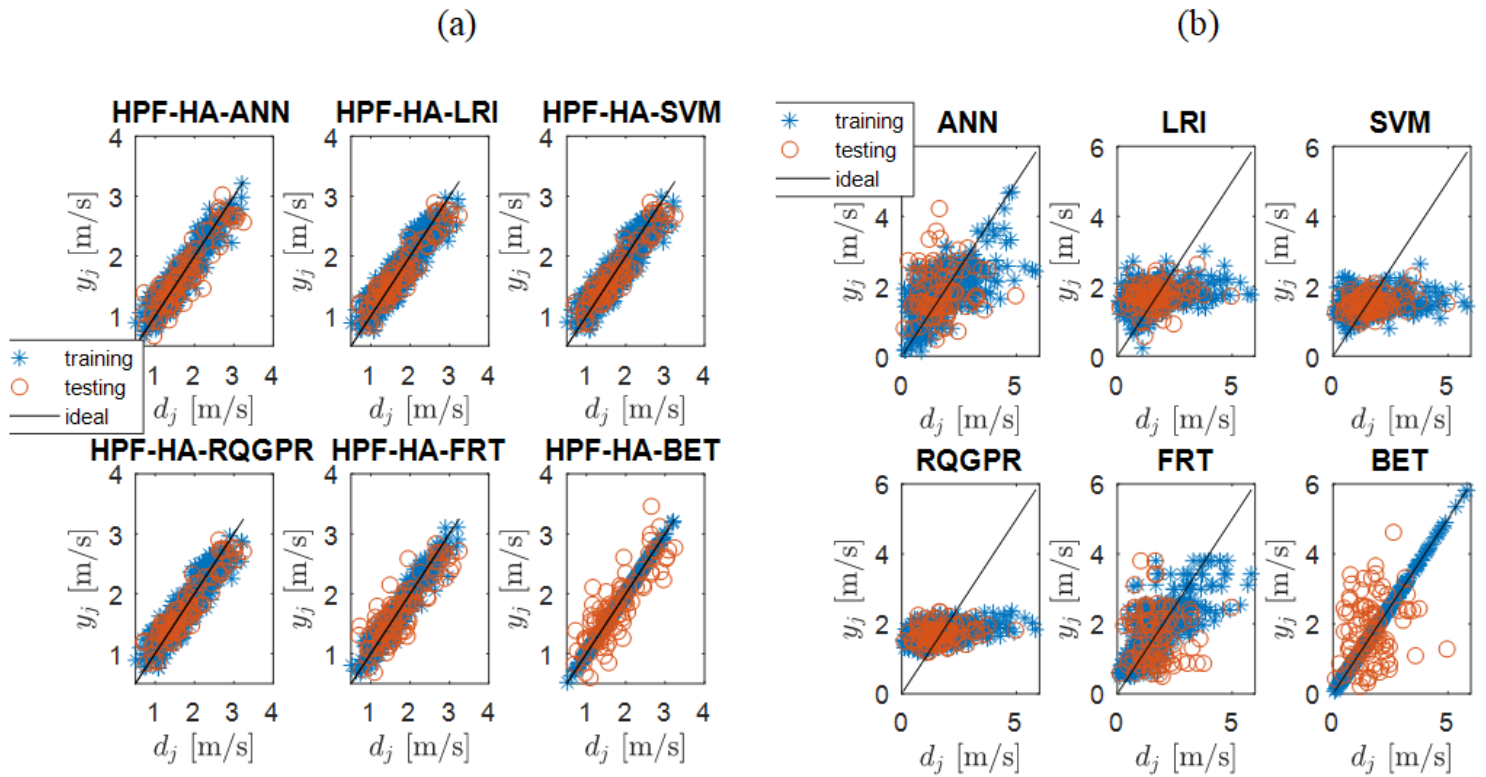


Figure 7

Plots of monthly wind speed predictions for Stuttgart (a) with HPF and HA pretreatments (b) without HPF and HA pretreatments

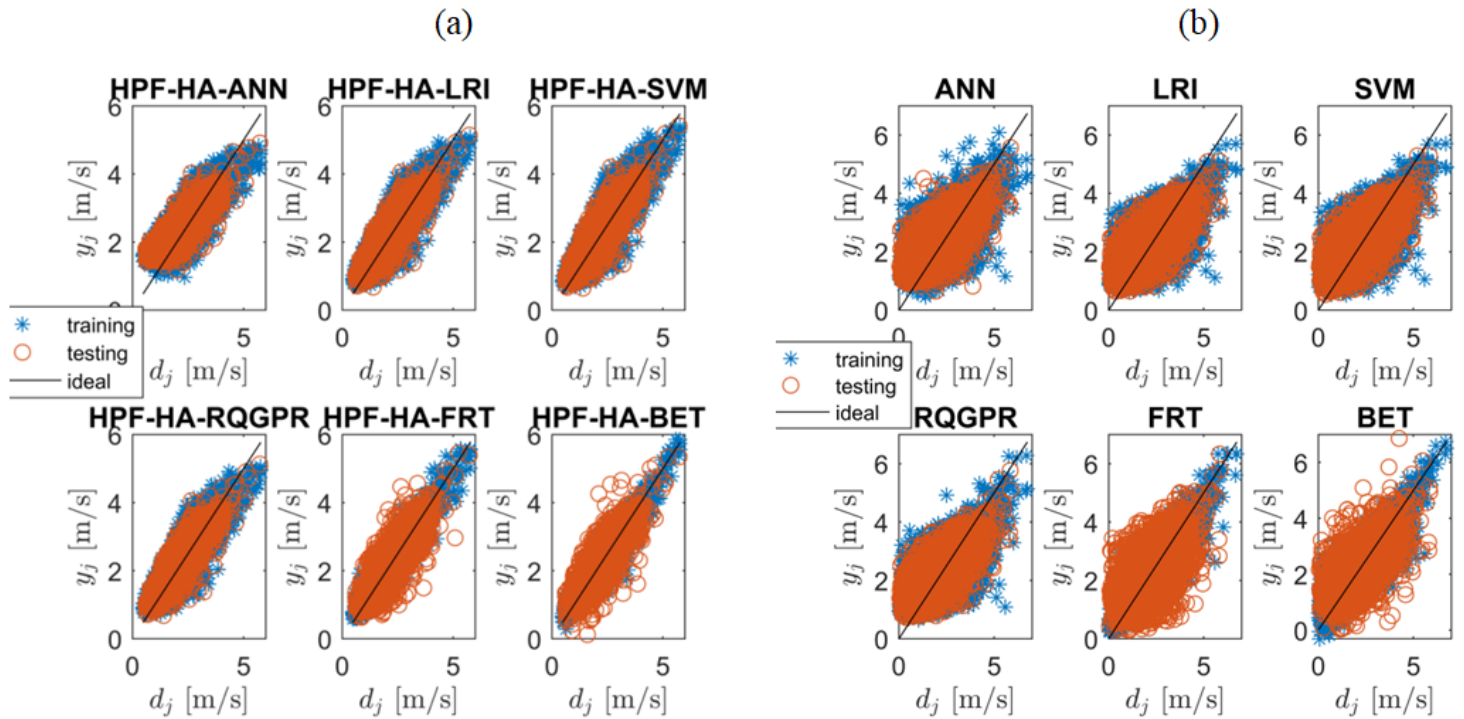


Figure 8

Plots of daily wind speed predictions for Enugu (a) with HPF and HA pretreatments (b) without HPF and HA pretreatments

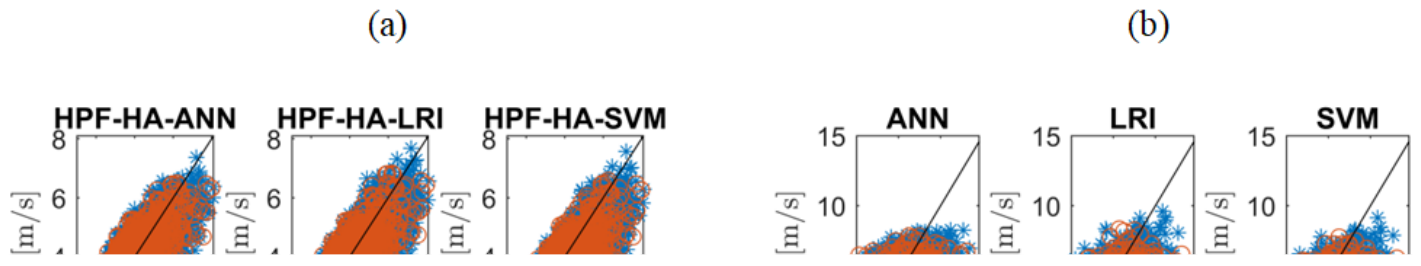


Figure 9

Plots of daily wind speed predictions for Stuttgart (a) without HPF and HA pretreatments (b) without HPF and HA pretreatments